Observer design for the Selective Catalytic Reduction of NOx in a loop reactor

This is an electronic version (author's version) of the paper:

Fissore D., Pisano R., Barresi A. A. (2007). Observer design for the Selective Catalytic Reduction of NOx in a loop reactor. Chemical Engineering Journal (Elsevier), 128(2-3), 181-189. DOI: 10.1016/j.cej.2006.09.026.

Observer design for the Selective Catalytic Reduction of NO_x in a loop reactor

Davide Fissore, *Roberto Pisano*, *Antonello A. Barresi*[*]

Dipartimento di Scienza dei Materiali ed Ingegneria Chimica, Politecnico di Torino, corso Duca degli Abruzzi 24, 10129 Torino (Italy)

[*] corresponding author: Davide Fissore, Dipartimento di Scienza dei Materiali ed Ingegneria Chimica, Politecnico di Torino, corso Duca degli Abruzzi 24, 10129 Torino (Italy), phone: +39-011-5644695, fax: +39-011-5644699, e-mail: davide.fissore@polito.it

Abstract

The aim of this work is to show how to design a soft-sensor to monitor the Selective Catalytic Reduction (SCR) of NO_x with NH_3 in a loop reactor, i.e. a loop-shape system made of N units with periodical variation of the feed position. The design procedure of Zeitz (1977) is used and, even if the design procedure remains basically heuristic, some general guidelines to design the observer are given. The proposed observer is demonstrated to allow for a quick and reliable estimation of the inlet NO_x concentration, as well as of the outlet reactants conversion and of the temperature profiles in the reactors, using some temperature measurements in the reactor, even when the NO_x and the NH_3 concentration in the feed change. The results may be used for control purposes, thus avoiding expensive hardware sensors and time consuming on-line measurements.

Keywords

Observer; state estimation; reactors network; loop reactor; chromatographic reactor; Selective Catalytic Reduction.

Introduction

Chemical Reaction Engineering is presently moving from conventional reactors, where only the chemical reaction takes place, to multifunctional units, where several operations, namely separation and/or heat exchange are coupled into a single equipment, resulting in higher yield and productivity and to lower investment and operation costs.

Among these multifunctional reactors, the chromatographic reactor, which couples chemical reaction and adsorptive separation, has received a great deal of attention as the continuous separation of products can drive a reversible reaction to near completion because of the suppression of the reverse reaction. Chromatographic operation can be achieved in a Reverse-Flow Reactor (RFR) packed with an adsorbent, or with a mixture of adsorbent and catalyst, with a high adsorption capacity toward a reactant and low toward a product, so that the periodic switching of the feed traps the strongly adsorbed reactant inside the reactor (see, for example, Agar & Ruppel (1988), Noskov et al. (1996) and Synder & Subramaniam (1998)). Moreover, in the RFR it is possible to exploit the thermal storage capacity of the catalytic bed, which can act as a regenerative heat exchanger, to allow auto-thermal behaviour when the adiabatic temperature rise of the feed is low (see, for example, the reviews of Matros & Bunimovich (1996) and Kolios, Frauhammer & Eigenberger (2000)). Nevertheless the RFR exhibits the problem of wash out, i.e. the emission of unconverted reactants occurring when the flow direction is reversed.

The Loop Reactor (LR), made of two or three reactors connected in a closed sequence with periodical variation of the feed position from one reactor to the following one in the sequence, can be considered an alternative device where no wash out can occur: a set of valves allows to change the feed position, thus simulating the behaviour of a moving bed and achieving a sustained dynamic behaviour. Contrary to the RFR, the flow direction is maintained, thus ensuring a uniform catalyst exploitation and avoiding wash out. The loop reactor was

investigated in presence of various reactions, namely the catalytic combustion of lean VOC mixtures (Brinkmann et al. (1999), Fissore & Barresi (2002)), the low pressure methanol synthesis (Velardi & Barresi (2002)) and the synthesis gas production (Fissore, Barresi & Baldi (2003)). Figure 1 shows a system made up of three reactors: acting on a set of valves (not shown in the figure) it is possible to change periodically the reactor sequence from the initial 1-2-3 to 2-3-1 and finally to 3-1-2.

The Selective Catalytic Reduction (SCR) of NO_x with NH_3 in presence of a catalyst that strongly adsorbs the ammonia was firstly suggested by Agar & Ruppel (1988) as a process which can be carried out in a RFR, taking advantage from this mode of reactor operation: isothermal operation was assumed in order to focus on the interaction between adsorption and chemical reaction. Fissore et al. (2006a) pointed out that even if the adiabatic rise in NO_x removal is usually of the order of 10-20 K, the temperature rise in a RFR will be a multiple of this value, thus allowing autothermal operation when low temperature gas is fed to the reactor. Moreover, Fissore et al. (2006a) compared the performance of the RFR and of a loop of three reactors evidencing that this second device allows to avoid the problem of wash out, beside achieving autothermal operation and fulfilling the constraints on the pollutant concentration in the product stream.

One of the main drawbacks which can limit the industrial application of this technology is that in addition to the intrinsically dynamic behaviour, one must deal with external perturbations (in the feed concentration, composition, temperature and flow rate) which may lead either to reaction extinction and thus to emission of unconverted pollutants and/or to catalyst overheating. This is particularly true in the case of the end-of-pipe treatment of combustion gas. It is thus necessary to implement some closed-loop control strategy based on the measurement of the inlet concentration (and composition), of the outlet conversion and of the temperature profile in the reactor. A model-based soft-sensor (observer) allows to estimate quickly and reliably the feed composition and the state variables profiles from some temperature measurements in the reactor, avoiding expensive hardware sensors and

time consuming on-line measurements. Soft-sensor stays for "software sensor" as the hardware of a physical sensor for a certain variable is replaced by a software which runs on a Personal Computer and returns the value of the desired variable. The observer combines the knowledge of the physical system (model) with experimental data (on-line measures) to provide on-line estimates of the sought states and/or parameters. The level of detail of the model is of straightforward importance in characterising the performance of the observer: if a detailed model taking into account finite reversal frequency and reaction kinetics is used, the resulting observer may be useless for the on line application, being too time-consuming for a computer; this motivates the research of simplified models to be used in the algorithm of the observer.

The problem of designing a full state observer for a chemical reactor, i.e. an observer which estimate all the variables which define the state of the system, namely the gas and solid temperature and composition, is about four decades old; anyway, the application of these techniques to an unsteady-state reactor (RFR or LR) is relatively new: Edouard et al. (2004) and Fissore et al. (2006b), among the others, designed an observer for a medium scale RFR where the autothermal combustion of lean VOC mixtures is carried out, using a simplified model which exploits the analogy between the RFR operated with high switching frequency and the countercurrent reactor (Nieken et al. 1995).

In the field of LR modelling, Sheintuch & Nekhamkina (2005) proposed two limiting pseudo-homogeneous models for a loop reactor with an infinite number of units: the first one corresponds to an arbitrary switching velocity, while the second corresponds to high switching frequency; they used a pseudo-homogeneous model to describe the loop reactor and a first order exothermic reaction. Fissore et al. (2006a) pointed out that high switching frequency is required in the loop reactor when the SCR of NO_x is carried out in order to achieve and maintain autothermal operation with low temperature feeding; thus the asymptotic model of Sheintuch & Nekhamkina (2005) will be used to design the observer in this work.

The paper is structured as follows: in Section 2 the mathematical model and the simplified model, based on the fast switching asymptote of Sheintuch & Nekhamkina (2005) will be formulated; in Section 3 the fundamentals of the observer design, based on the asymptotic model, are given, while the validation is given in Section 4. The design procedure of Zeitz (1977) is used and, even if the design procedure remains basically heuristic, some general guidelines to build the observer are given.

Detailed modelling of the Loop Reactor

A heterogeneous mathematical model is used to investigate the performance of the loop rector. An Eley-Rideal mechanism is used to describe the reaction between NO_x (A) in the gas phase and the ammonia (B) adsorbed on the catalyst:

$$A + B_S \rightarrow C \tag{1}$$

$$B + S \rightarrow B_S \tag{2}$$

The kinetic model proposed by Tronconi at al. (1996) for a V_2O_5/TiO_2 catalyst (with V_2O_5 loading of 1.47%) is used; the reduction reaction is considered to be of first order with respect to each reactants:

$$r_{red} = -k_{red} c_{A,i} \theta_B \Omega \tag{3}$$

where θ_B is the ammonia surface coverage and $c_{A,i}$ is the concentration of reactant A at the gas-solid interface. The adsorption rate of ammonia on the catalyst surface is assumed to be proportional to the ammonia concentration in the gas phase and to the free fraction of surface sites:

$$r_{ads} = k_{ads} c_{B,i} \left(1 - \theta_B\right) \Omega \tag{4}$$

while the rate of desorption is assumed to be proportional to the concentration of the adsorbed species:

$$r_{des} = k_{des} \theta_B \Omega \tag{5}$$

The kinetic model of Tronconi et al. (1996) invokes a Temkin-type desorption

isotherm, where the activation energy for desorption is a function of the surface coverage:

$$E_{a,des} = E_{a,des}^{\zeta}\left(1-\gamma\theta_B^{\sigma}\right) \tag{6}$$

An Arrhenius type dependence of the kinetic constants k_{red}, k_{ads} and k_{des} from the temperature is assumed

$$k_{red} = k_{0,red}e^{-\frac{E_{a,red}}{RT_S}},\ k_{ads} = k_{0,ads}e^{-\frac{E_{a,ads}}{RT_S}},\ k_{des} = k_{0,des}e^{-\frac{E_{a,des}}{RT_S}} \tag{7}$$

The SCR reaction is assumed to take place in a monolithic reactor: mass and energy dispersive transport are not taken into account, due to the low conductivity of the monolithic support, and also pressure loss inside the reactor is neglected; adiabatic operation is assumed. Thus, the system of partial differential equation that describes the process dynamics is the following:

- gas phase mass balance:

$$\frac{\partial c_A}{\partial t} = -v_G\frac{\partial c_A}{\partial z} + h_A a_v\left(c_{A,i}-c_A\right) \tag{8}$$

$$\frac{\partial c_B}{\partial t} = -v_G\frac{\partial c_B}{\partial z} + h_B a_v\left(c_{B,i}-c_B\right) \tag{9}$$

- solid phase mass balance:

$$\Omega\frac{\partial \theta_B}{\partial t} = r_{ads} - r_{des} - r_{red} \tag{10}$$

- gas phase energy balance:

$$\frac{\partial T_G}{\partial t} = -v_G\frac{\partial T_G}{\partial z} + \frac{h_T a_v}{\rho_G c_{p,G}}\left(T_G - T_S\right) \tag{11}$$

- solid phase energy balance:

$$\rho_S c_{p,S}\left(1-\varepsilon\right)\frac{\partial T_S}{\partial t} = -h_T a_v\left(T_S - T_G\right) + r_{red}\left(-\Delta H_{red}\right) + r_{ads}\left(-\Delta H_{ads}\right) + r_{des}\left(-\Delta H_{des}\right) \tag{12}$$

The value of $c_{A,i}$ and $c_{B,i}$, i.e. the gas concentration at the interface, are calculated from the mass balance at the gas-solid interface, assuming that there is no accumulation. Heat and mass transfer coefficients have been calculated using the asymptotic solution for a circular duct with fully developed concentration and temperature

profiles (see, for example, Skelland, 1974). The concentration of each reactant in the feed is the same, while the rest is inert gas; the catalyst is pre-heated to a uniform temperature of 600 K. The other operating conditions are given in Table 1.

The system of partial differential equations (8) - (12) is solved by discretising the domain of the spatial variable z into a grid of 60 points, equally spaced, thus obtaining a grid-independent solution. The MatLAB solver ode15s, which consists of a quasi-constant implementation of the Numerical Differentiation Formulas in terms of Backward Differences (Shampine & Reichelt, 1997) is used to solve the system; the relative and absolute tolerances are set equal to the square root of the working machine precision. After a transient period, the solution of the system evolves towards a periodic-steady state (PSS): the behaviour of the reactor (temperature and concentration profiles) is the same within every cycle. This model has been recently proven to be effective in describing the dynamic behaviour of the SCR in a LR (Fissore et al., 2006c).

Fast Switching Asymptote

Following the approach by Sheintuch and Nekhamkina (2005), a loop reactor of N identical units, each one of the length $\Delta L=L/N$ with gradual switching of the inlet/outlet ports at every time interval t_c is considered as an asymptote of the loop reactor. The boundary conditions are applied at positions that vary in time as stepwise functions with a total period $\lambda=N\cdot t_c$:

$$z_{in} = (n-1)\cdot\Delta L \text{ when } t \in \left[(n-1)t_c + s\lambda, nt_c + s\lambda\right] \quad n = 1,...,N \quad s = 0,1,... \tag{13}$$

where n identifies the number of the reactor of the loop and s the cycle.

As it has been pointed out in the Introduction, fast switching is required to allow autothermal operation; thus the switching velocity v_{sw} defined as:

$$v_{sw} = \frac{\Delta L}{t_c} = \frac{L}{N\cdot t_c} \tag{14}$$

is considered to be significantly faster than the gas velocity and the period λ is

assumed to be smaller than all other characteristic time scales, namely the characteristic time for convection, adsorption, desorption and reduction reaction. So, it is possible to define the switching cycle-averaged variables $\overline{c}_A(t,z)$, $\overline{c}_B(t,z)$, $\overline{T}_{G,0}(t,z)$ and, in the limit of many ports and fast switching, the axial profiles of c_A, c_B, T_G are continuous.

Let's consider the enthalpy balance during time interval $t_f \gg \lambda$ for a control volume of the length $\Delta L=L/N$ which combines two halves of adjacent reactor:

$$\left\{T_G\left(t+t_f\right)-T_G(t)\right\}\rho_G c_{p,G} S\Delta L = \left\{q_1 - q_2 + q_{in} - q_{out} - q_{ex}\right\} t_f \tag{15}$$

where:

- q_1 and q_2 are the heat flows entering and exiting from the volume $S\Delta L$ by convection:

$$q_1 - q_2 = v_G \rho_G S c_{p,G}\left(T_{G,1} - T_{G,2}\right) \tag{16}$$

- q_{in} and q_{out} are the heat flow of the feed and of the product extracted from the reactor:

$$q_{in} - q_{out} = v_G \rho_G S c_{p,G}\left(T_{G,0} - T_G\right) \qquad \text{if} \qquad 0 < t < t_c \tag{17}$$

otherwise this term is equal to zero as the intermediate part of the control volume acts as the inlet/outlet during the short time interval t_c;

- q_{ex} is the heat flow exchanged with the solid:

$$q_{ex} = h_T a_v S\Delta L\left(T_G - T_S\right) \tag{18}$$

In the limit $\lambda \to 0$ and $\Delta L \to 0$ the energy balance for the gas phase takes this form:

$$\frac{\partial \overline{T}_G}{\partial t} = -v_G \frac{\partial \overline{T}_G}{\partial z} + \frac{h_T a_v}{\rho_G c_{p,G}}\left(\overline{T}_G - \overline{T}_S\right) - \frac{v_G}{L}\left(\overline{T}_G - \overline{T}_{G,0}\right) \tag{19}$$

Similarly, this procedure can be applied also to the mass balance of NO_x and NH_3 for the same control volume, thus leading to these equations:

$$\frac{\partial \overline{c}_A}{\partial t} = -v_G \frac{\partial \overline{c}_A}{\partial z} + h_A a_v\left(\overline{c}_{A,i} - \overline{c}_A\right) - \frac{v_G}{L}\left(\overline{c}_A - \overline{c}_{A,0}\right) \tag{20}$$

$$\frac{\partial \overline{c}_B}{\partial t} = -v_G \frac{\partial \overline{c}_B}{\partial z} + h_B a_v\left(\overline{c}_{B,i} - \overline{c}_B\right) - \frac{v_G}{L}\left(\overline{c}_B - \overline{c}_{B,0}\right) \tag{21}$$

The last terms in eq. (19)-(21) shows that the discrete supply/removal acting at each port of a finite unit system during a short interval is incorporated into the limiting continuous model as permanently acting distributed source/sink terms. The heat and mass balance equations for the solid can be written for the same control volume and are not changed with respect to eq. (10) and (12); obviously the value of the temperature is substituted by the integral mean.

For a fixed value of the gas flow rate (and thus of the gas velocity) and of the number of reactors, the lower is the switching time the better is the approximation obtained with the FSA. Figure 2 shows that for a certain configuration of the network, in this case made up of three reactors, the error in the prediction of the gas species concentration profiles (lower graph) can exceed 100 % when the switching time is equal to 100 s; for lower values of the switching time (5-10 s) the agreement is much better and a high error is obtained only in the prediction of the gas phase composition in the first section of the reactor while the value of the outlet gas composition is correctly predicted (the agreement with the temperature profile, shown in the upper graph, is almost perfect). This is a consequence of the fact that the FSA give reliable predictions only when the value of the switching time is low.

Observer design

From a theoretical point of view a real-time simulation, based on a detailed model, can be used for the on-line estimation of the unmeasured temperature and concentration profiles of the loop reactor, but this simulation in unable to compensate for errors of the initial conditions, unknown disturbances, model parameters uncertainties and measurement errors. Therefore it is necessary to design a state estimator based on some temperature measurements (easy to be obtained) and an appropriate model.

Let us consider the following general non-linear system:

$$\dot{x} = f(x,u) \tag{22}$$

with observations given by

$$y = d^T x \tag{23}$$

where x is the state of the system, u is the input (manipulated) and y is the output of the system (made up of the measured variables); f is a non-linear function vector and d is a constant vector. In our process the vector x has the following structure:

$$x = \left[T_G(1),...,T_G(N),T_S(1),...,T_S(N),c_A(1),...c_A(N),c_B(1),...,c_B(N),...,\theta_B(1),...,\theta_B(N)\right]^T \tag{24}$$

where N is the number of points used to discretise the mass and energy balance equations, while y is a vector made up of the measured variables and u is made up of all the variables that can be manipulated, i.e. the switching time and the inlet temperature.

Due to the strongly non-linear characteristics of the system under investigation, the state estimation approaches, based on linearization techniques and lumping (via the orthogonal collocation method) that are usually adopted for non-linear distributed parameter fixed bed reactors, are not suitable. Moreover, the application of the extended Kalman filter to the full non-linear distributed parameters model of the reactor results in a large number of differential equations (Windes et al., 1989) and the computational effort is considerably increased. Therefore the design concept of Zeitz (1977), which is an extension of the classical Luenberger observer, is used to calculate the observer gain: in order to estimate the unknown state x using the known information y and u, we consider the following nonlinear observer:

$$\dot{\hat{x}} = f(\hat{x},u) + K(\hat{x},u)(y - \hat{y}) \tag{25}$$

The observer is derived from the model equation by adding a suitable term which consists of the errors between the measured states and the observed ones multiplied by the gain K, which is a non-linear function matrix with respect to the state and input of the observer. The state of the observer is thus made up of the values of the solid and gas temperatures, as well as the concentrations of A and B in the gas phase

and on the catalyst surface (see eq. (24)).

Let us define the observation error:

$$e = x - \hat{x} \tag{26}$$

The following differential equation results after subtraction of eq. (22) and (25):

$$\dot{e} = \dot{x} - \dot{\hat{x}} = f(x,u) - f(\hat{x},u) - K(\hat{x},u)d^T e \tag{27}$$

Linearization yields:

$$\dot{e}|_{\hat{x}} = \left(\left.\frac{\partial f}{\partial x}\right|_{\hat{x}} - K(\hat{x},u)d^T \right) e \tag{28}$$

If the gain is chosen as:

$$K(\hat{x},u)d^T = \left.\frac{\partial f}{\partial x}\right|_{\hat{x}} + \kappa I \tag{29}$$

where κ is a positive tuning parameter, then the observation error is described by the following homogeneous differential equation:

$$\dot{e}|_{\hat{x}} = (-\kappa I)e \tag{30}$$

When the parameter κ is properly selected, the solution of eq. (30) will asymptotically tend to zero, thus ensuring the convergence of the estimated state $\hat{x}$ to the real one x. The important advantages of this method are its feasibility for general non-linear problems, the possibility to use physical considerations in the design process, as well as its availability for on-line implementation. A very similar approach was used, among the others, by Hua et al. (1998) for the estimation of the temperature and concentration profiles in a circulation loop reactor where the autothermal combustion of lean VOC mixtures is carried out.

In order to reduce the complexity of the model and since an observer can compensate for some model uncertainties, the asymptotic model previously described was used for the observer development; the FSA was further simplified by neglecting the mass transfer resistance between the solid and the gas phase. The feed temperature and the feed flow rate are assumed to be known, as well as the feed composition and some temperature measurements:

$$y(t) = \left[T_S(z_1, t), ..., T_S(z_m, t) \right]^T \tag{31}$$

where the superscript T denotes the transpose of the vector and m is the number of measurement points in the reactor (a second observer will be designed in the second part of the paper with the aim to estimate also the feed concentration).

For a linear distributed parameter system, the gain of its observer is only a function of the spatial variable. In our case the gain of the obtained non-linear distributed parameter observer is non-linear due to the term $\left.\frac{\partial f}{\partial x}\right|_{\hat{x}}$ in eq. (29). Some simulation studies showed that these terms are zero, apart from some narrow peaks, thus they have only a weak influence on the asymptotic stability of the observer and will be neglected in the following, thus leading to:

$$K(\hat{x}, u) c^T = \left.\frac{\partial f}{\partial x}\right|_{\hat{x}} + \kappa I \cong -\alpha I \tag{32}$$

which means that the observer equation becomes:

$$\dot{\hat{x}} = f(\hat{x}, u) + K(\hat{x}, u)(y - \hat{y}) \cong f(\hat{x}, u) - \alpha e \tag{33}$$

Thus, the objective of the observer design is now to determine the tuning parameter α such that the observation error tends asymptotically and rapidly to zero for all relevant initial errors. Moreover, the rate of convergence is also determined by this parameter. Different values of α can be used as a function of the axial coordinate, but this is not necessary in our application as it will be shown by the subsequent results.

Actually, eq. (33) requires the errors e to be known all the reactor long, i.e. in all the axial coordinate z where the equations are discretised, but they are known only for the m points were the solid temperature is measured. Here, according to the method proposed by Mangold et al. (1994), exponential weighting functions will be used to approximate the error profiles:

$$\hat{T}_S(z, t) - T_S(z, t) \cong \sum_{k=1}^{m} \left(\hat{T}_S(z_k, t) - T_S(z_k, t) \right) w_k(z) \tag{34}$$

where:

$$w_k(z)=\begin{cases}\exp\left(-\dfrac{z_k-z}{\beta(z_{k-1}-z_k)}\right) & z_{k-1}<z_k\le z_{k+1}\\ 0 & \text{otherwise}\end{cases} \tag{35}$$

with β positive adjustable parameter. The validity of eq. (35) stays in the fact that the observation errors are small immediately behind a sensor locations and they increase with increasing distance from the next sensor location in flow directions.

As there are no concentration measurements available in the reactor, the error in the solid temperature predictions (e) will be used to correct also the mass balances, thus considering the concentration profile to be dependent on the temperature value. Thus, the equations of the observer take the form:

$$\begin{cases}\dot{\hat{T}}_G = f_1(T_G,T_S,c_A,c_B,\theta_B,u)-\alpha_t e\\ \dot{\hat{T}}_S = f_2(T_G,T_S,c_A,c_B,\theta_B,u)-\alpha_t e\\ \dot{\hat{c}}_A = f_3(T_G,T_S,c_A,c_B,\theta_B,u)-\alpha_{c,1} e\\ \dot{\hat{c}}_B = f_4(T_G,T_S,c_A,c_B,\theta_B,u)-\alpha_{c,2} e\\ \dot{\hat{\theta}}_B = f_5(T_G,T_S,c_A,c_B,\theta_B,u)-\alpha_{c,3} e\end{cases} \tag{36}$$

where different values of α will be used in the mass balance equations (and it will be referred as α_c) and in the energy balances (α_t). Finally, the design of the observer for our process reduces to choose carefully the values of the parameters β, α_t and α_c.

Observability and choice of sensor locations

If the system is observable and the gains are properly designed, the observer states converge to the true state of the system. Hence, it is important to select the location of the sensors in such a way to guarantee the observability of the loop reactor. Observability is a structural property of a system requiring that all states are reflected in the measurements differently. In traditional fixed-bed reactors the reaction zone extends in a small fraction of the reactor length, thus only temperature measurements within this zone can guarantee observability of the temperature profile. As the concentration profile is coupled strongly to the temperature profile, it

seems reasonable that if the temperature profile is observable, the concentration profile is also observable. In the loop reactor the temperature (and concentration) profiles migrate along the reactor and the reaction zone pass every temperature sensors at any location during one period, thus the reactor is observable over its whole length and the choice of sensors locations is arbitrary.

Actually, as the FSA is used to design the observer, the loop reactor is assumed to be a fixed-bed with distributed source/sink terms and thus sensor locations have to be carefully chosen. Temperature measurements should be taken in points which exhibits the larger and faster response to any change in the operating conditions. To this purpose we have considered how the solid temperature profiles change as a function of the inlet concentration. Figure 3 (upper graph) shows the results obtained when the PSS has been reached, pointing out that the points at $z = \frac{L}{12}, \frac{5L}{12}, \frac{3L}{4}$ are those that exhibit a larger variation and thus can be good candidate for our observer. This conclusion is confirmed by Figure 3 (lower graph) where the time evolution of the solid temperature at various axial position after step changes in the feed composition are given: again, the temperature at $z = \frac{L}{12}, \frac{5L}{12}, \frac{3L}{4}$ are those which exhibits a faster response, and thus will be used to design the observer.

Figure 4 shows an example of the solid temperature profiles predicted by an observer with the three previously chosen measurement points. It comes out that the errors in the predictions of the observer are in the range ±2 % for most of the reactor length (so that the observer is able to estimate correctly the maximum temperature), but the prediction of the temperature in the first part of each bed is quite poor (error > 20%). If the number of temperature measurements is increased to six, using also the values of the temperatures at the entrance of each reactor (which can be easily measured), the accuracy of the prediction is substantially improved and the difference between the temperature profile predicted by the observer and the "true" values (predicted by the detailed model) vanishes.

Tuning of the design parameters

The observer equations contain two design parameters, namely the gain α and the weight β. Actually, as only the error in the estimation of the solid temperatures is available from the measurements and this error is used to correct also the mass balances, two values of the gain, namely α_t and α_c have been used to correct the energy and the mass balances respectively. Usually the parameter α determines the convergence of the observer; in our case a suitable range of α is from 10 to 10^5. Figure 5 (upper graph) shows the results that can be obtained using different values of α_t: the evolution of the solid temperature in a certain position is given as predicted by the detailed model and by the observer. It must be pointed out that the observer has been initialised with a temperature and concentration profile different from that of the detailed model. Due to the features of the process (high thermal inertia) the influence of the parameter tuning in the above ranges on the observer performance is not very high. The same conclusions arise as far as the parameter α_c is concerned (Figure 5, lower graph). With regard to this parameter we have to remark that, due to numerical instabilities, a different gain ($\alpha_{c,2}$) should be used to correct the mass balance equation for the reactant B, while the same value can be used for the mass balances of reactants A and C. In all the simulations the error in the predictions of the observer in lower than 1%.

A proper choice of β is helpful for improving the approximation accuracy of the observation error profiles. Here β should range from 0.1 to 0.8, following the indication of Hua et al. (1998), but, similarly to what pointed out concerning the gain α, the influence of this parameter is quite weak (see Figure 6) and the error in the predictions is always less than 1%; a value of $\beta = 0.5$ will be used in the subsequent.

Estimation of the feed composition

Beside the estimation of the temperature and concentration profiles (and thus of the pollutant emissions), the problem of the estimation of the inlet pollutant concentration has to be investigated. Eq. (33) allows in fact to estimate the

concentration and temperature profiles, but requires to know the value of the feed flow rate (which can be easily measured) and of the feed composition. Although, in some cases, concentration analysers are installed, they are usually expensive to operate and maintain, and they have relatively slow sampling rates. Therefore the possibility of exploiting the observer to get estimation of the feed composition has to be addressed. The approach we propose is quite simple: we set the initial concentration $c_{A,0}$ as a new state variable in an expanded system, and then design a non-linear state observer. Following the common practice in industry, we assume that the unknown inlet concentration can be described by a simple disturbance model:

$$\dot{c}_{A,0} = \xi(t); \quad \xi(0) = c_{A,in} \tag{37}$$

where $\xi(t)$ is assumed to be an unknown, but bounded function. There are many studies focused on this problem, but the available results are too problem-dependent, suitable for a very restricted class of non-linear systems (Soroush, 1997). The observability and the convergence of the observer have been discussed, among the others, by Farza et al. (1997). When $\xi(t)=0$ some researcher showed that the estimation error converges exponentially to zero (Deza et al., 1992). Here, according to the common practice in the industrial process, we assume $\xi(t)=0$ and use an extended Luenberger observer:

$$\dot{c}_{A,0} = K_2\left(y - \hat{y}\right) \tag{38}$$

where K_2 is the gain of the observer which has to be chosen in order to meet the general requirements on an observer, i.e. asymptotic stability and fast convergence to the real states. The structure of the observer which predicts the evolution of the temperature and of the concentration remains unchanged; the same temperature measures are used in this case. Figure 7 evidences the results obtained when the inlet concentration of both reactants is increased (upper graph) and decreased (lower graph). An optimal value of K_2 = 10 is found which ensures fast and accurate predictions of the observer: no steady-state error is obtained; higher values of this

gain worsen the prediction as well as the speed of the response. After the transient the error in the prediction, if present, remains almost constant and is a function of the observer gain.

Conclusion

The control of a loop reactor where the Selective Catalytic Reduction of NO_x with NH_3 requires to know both the solid temperature (to prevent catalyst overheating) and the NO_x and the NH_3 conversion (to avoid pollutant emission). The proposed observer was demonstrated to give a quick and reliable estimation of the solid temperature and of the pollutant conversion, using some temperature measurements. A simplified model, valid for high switching frequency, was used to design the observer. This does not constitute a limitation of the proposed algorithm as fast switching is required to get autothermal behaviour when feeding low temperature reactants. General guidelines to select the optimal sensor locations and the values of the parameters of the observer have been discussed.

This instrument can also be used in a state-space based control framework (like LQR or MPC); this kind of control algorithms is different from the more traditional feedback control loop as the control action is a function of all the states of the system (temperature and composition profiles) and not only of the values of the temperature and/or composition in the stream leaving the reactor. This allows to introduce the concept of "optimisation" in the calculation of the control action: in both LQR and MPC algorithms the value of the manipulated variables is in fact found by minimising a certain objective function. This will be the subject of a future work.

Notation

a_v	specific surface of the catalyst, m^{-1}
c	gas phase concentration, mol m^{-3}
c_p	specific heat, J kg^{-1} K^{-1}
d	constant vector
e	estimation error
E_a	activation energy, J mol^{-1}
h_i	mass transfer coefficient for the i-th species, m s^{-1}
h_T	heat transfer coefficient, J m^{-2} s^{-1} K^{-1}
$-\Delta H$	heat of reaction, J mol^{-1}
K	observer gain
k_{ads}	adsorption rate constant, m^3 mol^{-1} s^{-1}
k_{des}	desorption rate constant, s^{-1}
k_{red}	reduction rate constant, m^3 mol^{-1} s^{-1}
$k_{0,ads}$	frequency factor of the adsorption rate constant, m^3 mol^{-1} s^{-1}
$k_{0,des}$	frequency factor of the desorption rate constant, s^{-1}
$k_{0,red}$	frequency factor of the reduction rate constant, m^3 mol^{-1} s^{-1}
L	total reactor length, m
ΔL	length of each reactor of the loop, m
m	number of measurements in the reactor
n	number of the reactor in the loop
N	total number of reactors in the loop
q_{ex}	heat flow exchanged with the solid, J
q_{in} (q_{out})	heat flow of the feed (product) stream, J
q_1 (q_2)	heat flow entering (exiting) from the volume $S\Delta L$ by convection, J
Q	gas flow rate, Nl min^{-1}
r	rate of reaction, mol s^{-1} m^{-3}
R	ideal gas constant, J K^{-1} mol^{-1}
s	number of cycles

S	cross section area, m^2
t	time, s
t_c	switching time, s
t_f	time interval, s
T	temperature, K
u	input vector
v_G	gas velocity, m s^{-1}
v_{sw}	switching velocity, m s^{-1}
x	state vector
y	output (measurements) vector
w	weighting functions
z	spatial coordinate, m

Greeks

α	simplified gain of the observer
β	coefficient of weighting functions
γ, σ, ζ	parameters for the surface coverage dependence of $E_{a,\,des}$
ε	monolith void fraction
θ	surface coverage
κ	tuning parameter of the observer
λ	period of the operation, s
ρ	density, kg m^{-3}
ξ	bounded function
Ω	catalyst capacity, mol m^{-3}

Subscripts and Superscripts

(overlay)	average over a time interval larger than the period λ
^	estimate
0	feeding condition

A, B	reactants
ads	adsorption reaction
des	desorption reaction
G	gas phase
i	value at the gas-solid interface
in	inlet position
red	reduction reaction
S	solid phase

Abbreviations

FSA	Fast Switching Asymptote
LR	Loop reactor
LQR	Linear Quadratic Regulator
MPC	Model Predictive Control
PSS	Periodic Steady-State
RFR	Reverse Flow Reactor
SCR	Selective Catalytic Reduction

References

Agar, D. W., & Ruppel, W. (1988). Extended reactor concept for dynamic DeNOx design. *Chemical Engineering Science*, 43, 2073-2078.

Brinkmann, M., Barresi, A. A., Vanni, M., & Baldi, G. (1999). Unsteady-state treatment of very lean waste gases in a network of catalytic burners. *Catalysis Today*, 47, 263-277.

Deza, F., Busvelle, E., Gauthier, J. P., & Rakotopara, D. (1992). High gain estimation for nonlinear systems, *Systems Control Letters*, 18, 295-299

Edouard, D., Schweich, D., & Hammouri, H. (2004). Observer design for reverse flow reactor. *AIChE Journal*, 50, 2155-2166.

Farza, M., Hammouri, H., Othman, S., & Busawon, K. (1997). Nonlinear observers for parameters estimation in bioprocesses. *Chemical Engineering Science*, 52, 4251-4267

Fissore, D., & Barresi, A. A. (2002). Comparison between the reverse-flow reactor and a network of reactors for the oxidation of lean VOC mixtures, *Chemical Engineering Technology*, 25, 421-426.

Fissore, D., Barresi, A. A., & Baldi, G. (2003). Synthesis gas production in a forced unsteady state reactor network. *Industrial & Engineering Chemistry Research*, 42, 2489-2495.

Fissore, D., Barresi, A. A., & Botar-Jid, C. C. (2006a). NO_x removal in forced unsteady-state chromatographic reactors. *Chemical Engineering Science*, 61, 3409-3414.

Fissore, D., Edouard, D., Hammouri, H., & Barresi, A. A. (2006b). Non-linear soft-sensors design for unsteady-state VOC afterburners. *AIChE Journal*, 52, 282-291.

Fissore, D., Garran, D., & Barresi A. A. (2006c). Experimental investigation of the SCR of NO_x in a Simulated Moving Bed Reactor. *AIChE Journal*, 52, 3146-3154

Hua, X., Mangold, M., Kienle., A., & Gilles, E. D. (1998). State profile estimation of an autothermal periodic fixed-bed reactor. *Chemical Engineering Science*, 53, 47-58.

Kolios, G., Frauhammer, J., & Eigenberger, G. (2000). Authothermal fixed bed reactor

concepts. *Chemical Engineering Science*, 55, 5945-5967.

Mangold, M., Lauschke, G., Schaffner, J., Zeitz, M., & Gilles, E. D. (1994). State and parameter estimation for adsorption columns by nonlinear distributed parameter state observer. *Journal of Process Control*, 4, 163-172.

Matros, Y. H., & Bunimovich, G. A. (1996). Reverse flow operation in fixed bed catalytic reactors. *Catalysis Review-Science and Engineering*, 38, 1-68.

Nieken, U., Kolios, G. & Eigenberger, G. (1995). Limiting cases and approximate solutions for fixed-bed reactors with periodic flow reversal. *AIChE Journal*, 41, 1915-1925.

Noskov, A., Bobrova, L., Bunimovich, G., Goldman, O., Zagoriuko A., & Matros, Y. (1996). Application of the non-stationary state of catalyst surface for gas purification from toxic impurities. *Catalysis Today*, 27, 315-319.

Sheintuch, M., & Nekhamkina, O. (2005). The asymptotes of loop reactors. *AIChE Journal*, 51, 224-234.

Shampine, L. F., & Reichelt, M. W. (1997). The MatLab ode suite. *SIAM Journal on Scientific Computing*, 18, 1-22.

Skelland, A. H. P. (1974). *Diffusional Mass Transfer*. John Wiley & Sons Inc. New York.

Soroush, M. (1997). Nonlinear state-observer design with application to reactors. *Chemical Engineering Science*, 52, 387-404

Synder, J. D., & Subramanian, B. (1998). Numerical simulations of a reverse flow NOx-SCR reactor with side-stream ammonia addition. *Chemical Engineering Science*, 53, 727-734.

Tronconi, E., Lietti, L., Forzatti, P., & Malloggi, S. (1996). Experimental and theoretical investigation of the dynamics of the SCR-DeNOx reaction. *Chemical Engineering Science*, 51, 2965-2970.

Velardi, S. A., & Barresi, A. A. (2002). Methanol synthesis in forced unsteady-state reactor network. *Chemical Engineering Science*, 57, 2995-3004.

Windes, L. C., Cinar, A., & Ray, W. H. (1989). Dynamic estimation of temperature and concentration profiles in a packed bed reactor. *Chemical Engineering Science*,

44, 2087-2106.

Zeitz, M. (1977). PhD Thesis: *Nonlinear observers for chemical reactors*, VDI-Fortschr.-Ber., Reihe 8, No. 27, VDI-Verlag, Dusseldorf.

List of Tables

Table 1 Values of the main operating parameters used in the simulations.

$k_{0,red}$	$9.8 \cdot 10^{9}$ s^{-1}
$E_{a,red}$	77891 J mol^{-1}
$k_{0,ads}$	$3.4 \cdot 10^{5}$ m^{3} mol^{-1} s^{-1}
$E_{a,ads}$	37656 J mol^{-1}
$k_{0,des}$	$4.1 \cdot 10^{7}$ s^{-1}
$E_{a,des}^{\zeta}$	123428 J mol^{-1}
γ	0.315
σ	1.0
Ω	210 mol m^{-3}
ε	0.65
L	0.45 m
ρ_S	2500 kg m^{-3}
$c_{p,S}$	0.9 kJ kg^{-1} K^{-1}

List of Figures

$\alpha_t = 10^5$; other parameters of the observer: $\alpha_{c,1} = 10^4$, $\alpha_{c,2} = 10^{-1}$, $\alpha_{c,3} = 10^4$) and for different values of $\alpha_{c,1}$ (lower graph, –○– : $\alpha_{c,1} = 10$, –△– : $\alpha_{c,1} = 10^3$, –●– : $\alpha_{c,1} = 10^5$; other parameters of the observer $\alpha_{c,2} = \alpha_{c,1}$, $\alpha_t = 10^4$). Operating conditions: $Q_A = Q_B = 0.1$ Nl min^{-1}, $t_c = 10$ s, $c_{B,0} = c_{A,0}$ (the scenario of the inlet concentration is given in the small charts).

Figure 6 Comparison between the axial solid temperature profiles predicted by the detailed model (–□–) and by the observer for different values of β (----- $\beta = 0.2$, — · · — · : $\beta = 0.4$, — —: $\beta = 0.8$).
Operating conditions: $Q_A = Q_B = 0.1$ Nl min^{-1}, $t_c = 10$ s, $c_{B,0} = c_{A,0} = 5000$ ppmV, $\alpha_t = 10^4$, $\alpha_{c,1} = 10^4$, $\alpha_{c,2} = 10^{-1}$, $\alpha_{c,3} = 10^4$.

Figure 7 Comparison between the real values (dashed lines) and the predictions of the observer (symbols) of the inlet NO_x concentration (–Δ–: $K_2 = 10$, –O–: $K_2 = 10^2$, –□–: $K_2 = 10^4$).
Operating conditions: $Q_A = Q_B = 0.1$ Nl min^{-1}, $t_c = 10$ s, $c_{B,0} = c_{A,0}$, $\alpha_t = 10^4$, $\alpha_{c,1} = 10^4$, $\alpha_{c,2} = 10^{-1}$, $\alpha_{c,3} = 10^4$.

Figure 1

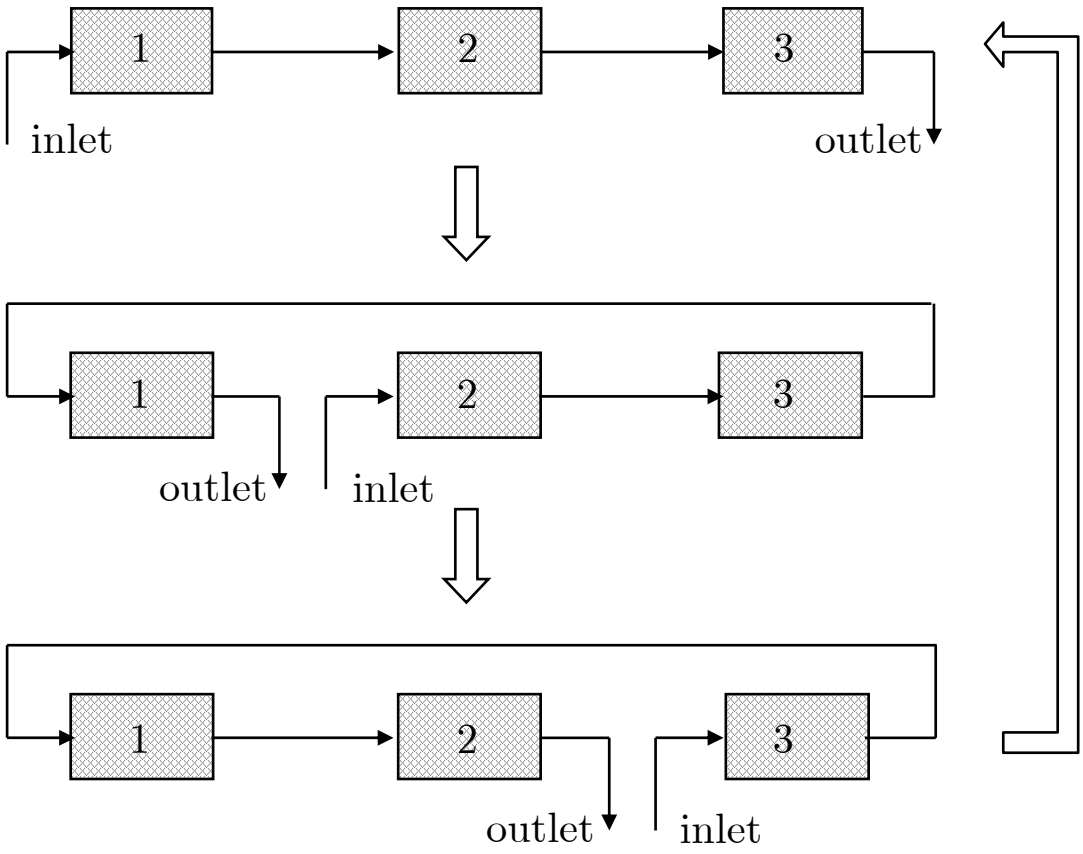

Figure 2

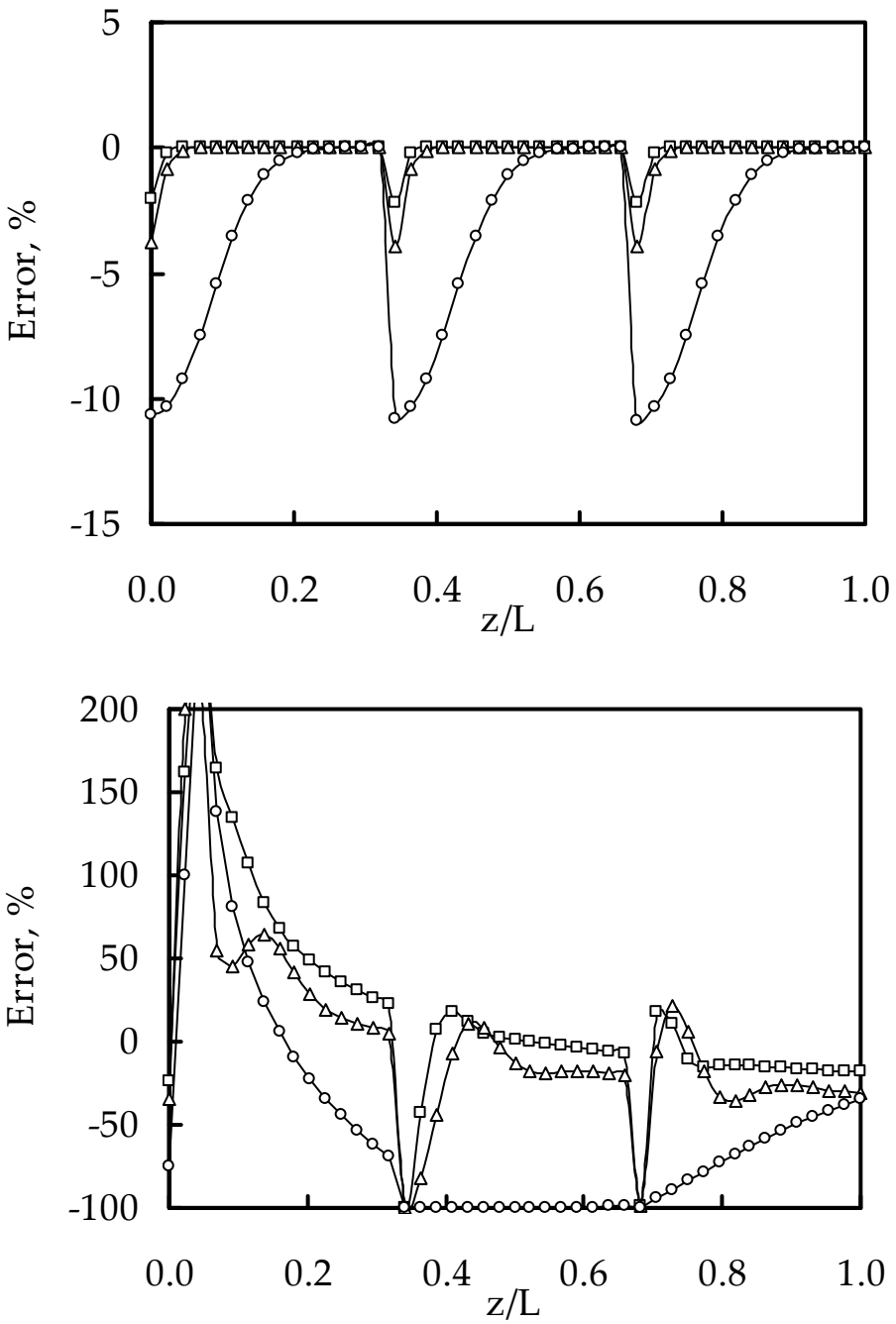
5
0
-5
-10
-15
Error, %
0.0
0.2
0.4
0.6
0.8
1.0
z/L
200
150
100
50
0
-50
-100
Error, %
0.0
0.2
0.4
0.6
0.8
1.0
z/L

Figure 3

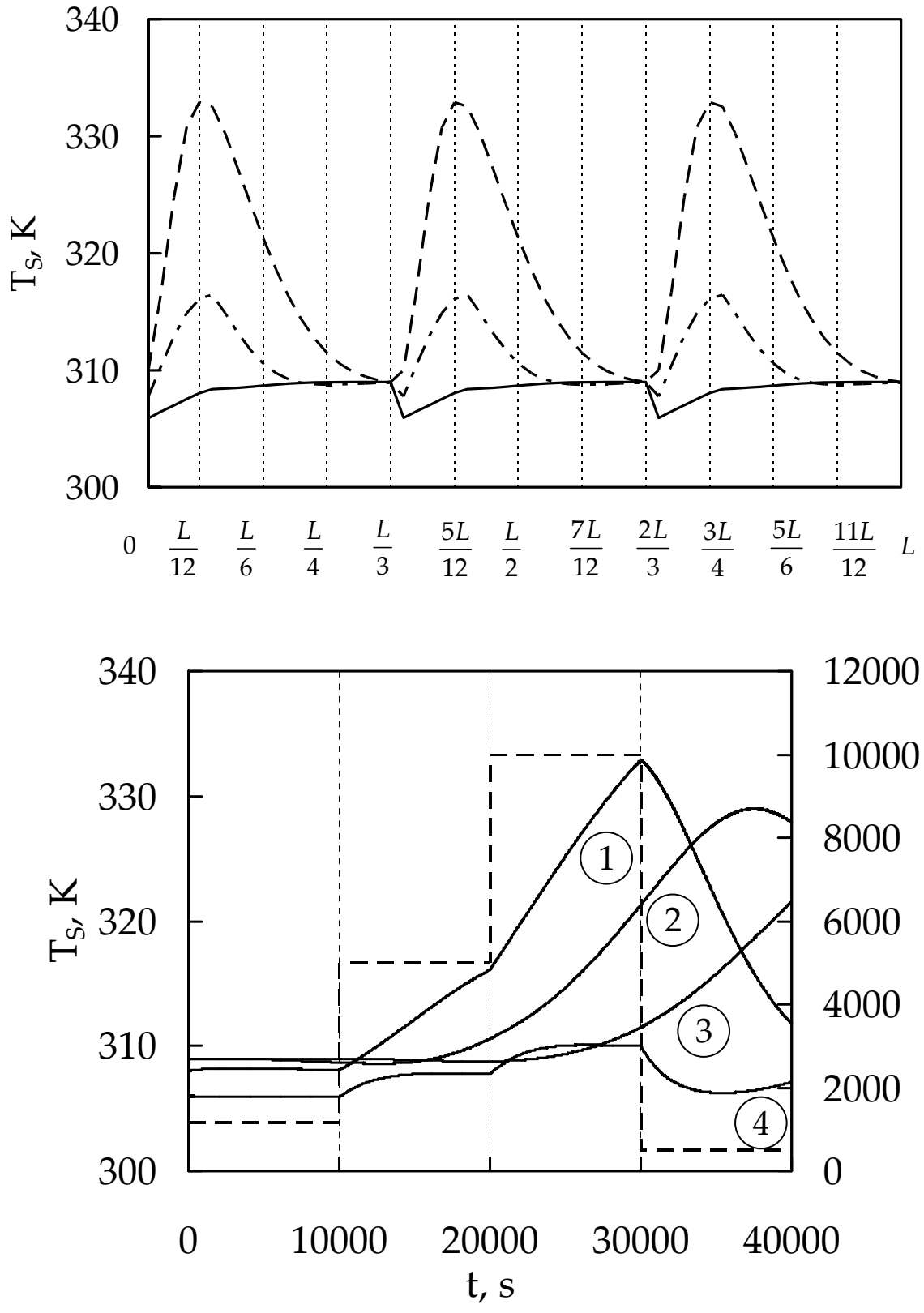
340
330
320
310
300
T_S, K
0
$\frac{L}{12}$
$\frac{L}{6}$
$\frac{L}{4}$
$\frac{L}{3}$
$\frac{5L}{12}$
$\frac{L}{2}$
$\frac{7L}{12}$
$\frac{2L}{3}$
$\frac{3L}{4}$
$\frac{5L}{6}$
$\frac{11L}{12}$
L
340
330
320
310
300
12000
10000
8000
6000
4000
2000
0
T_S, K
1
2
3
4
0
10000
20000
30000
40000
t, s

Figure 4

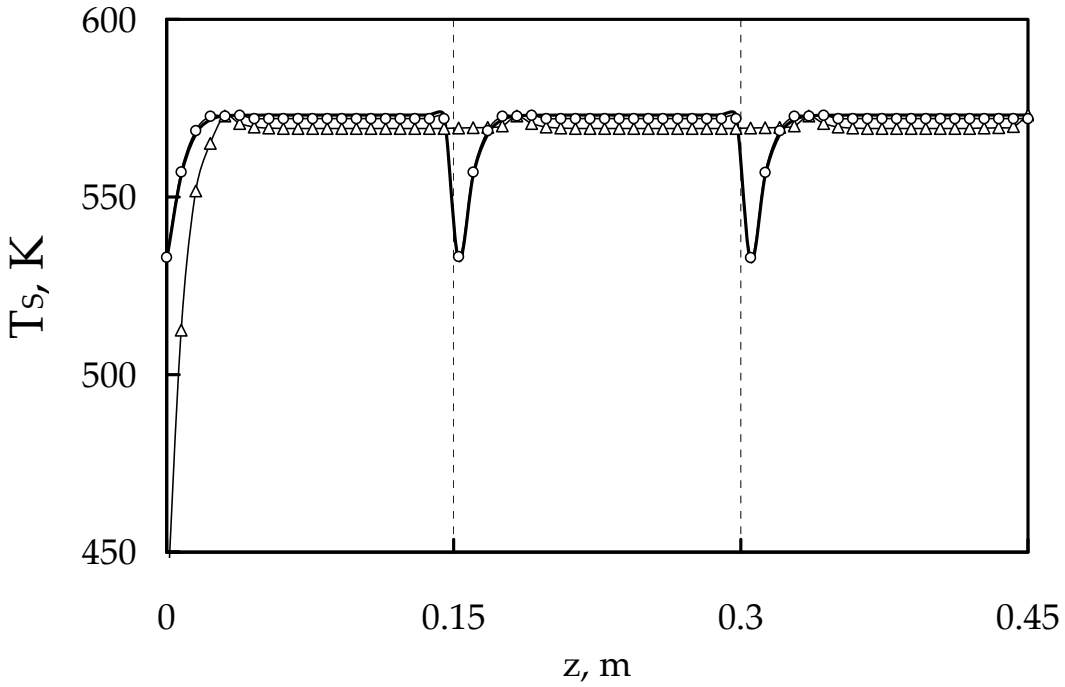

Figure 5

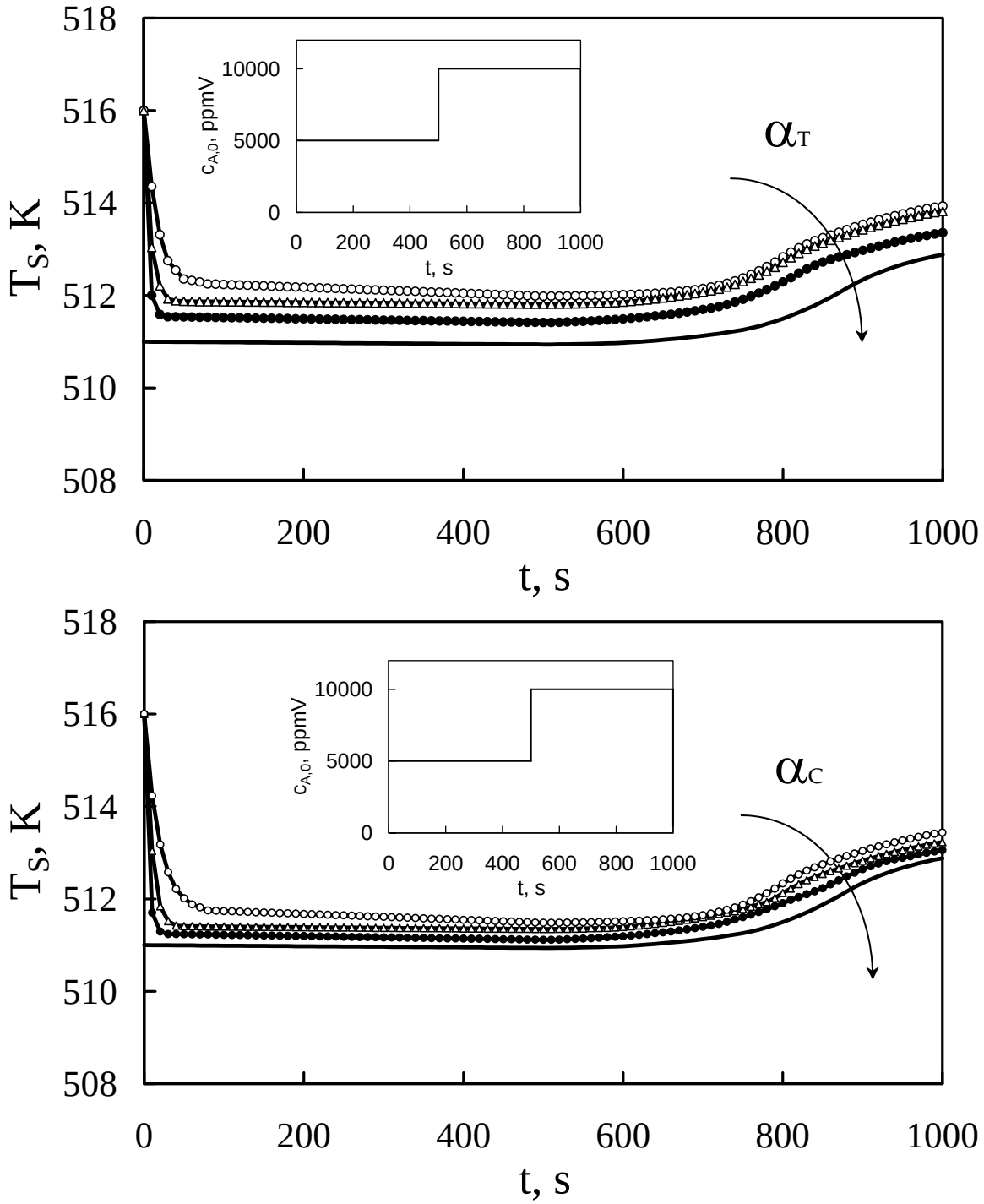
518
516
514
512
510
508
T_S, K
0
200
400
600
800
1000
t, s
α_T
10000
5000
0
$c_{A,0}$, ppmV
α_C

Figure 6

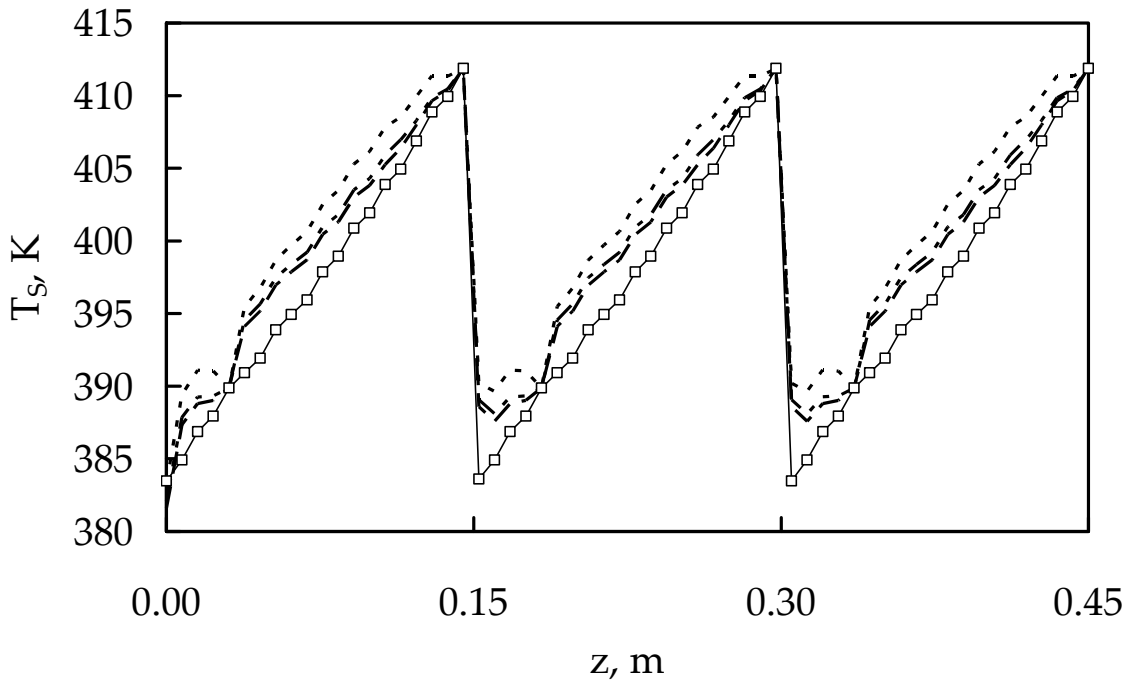

Figure 7

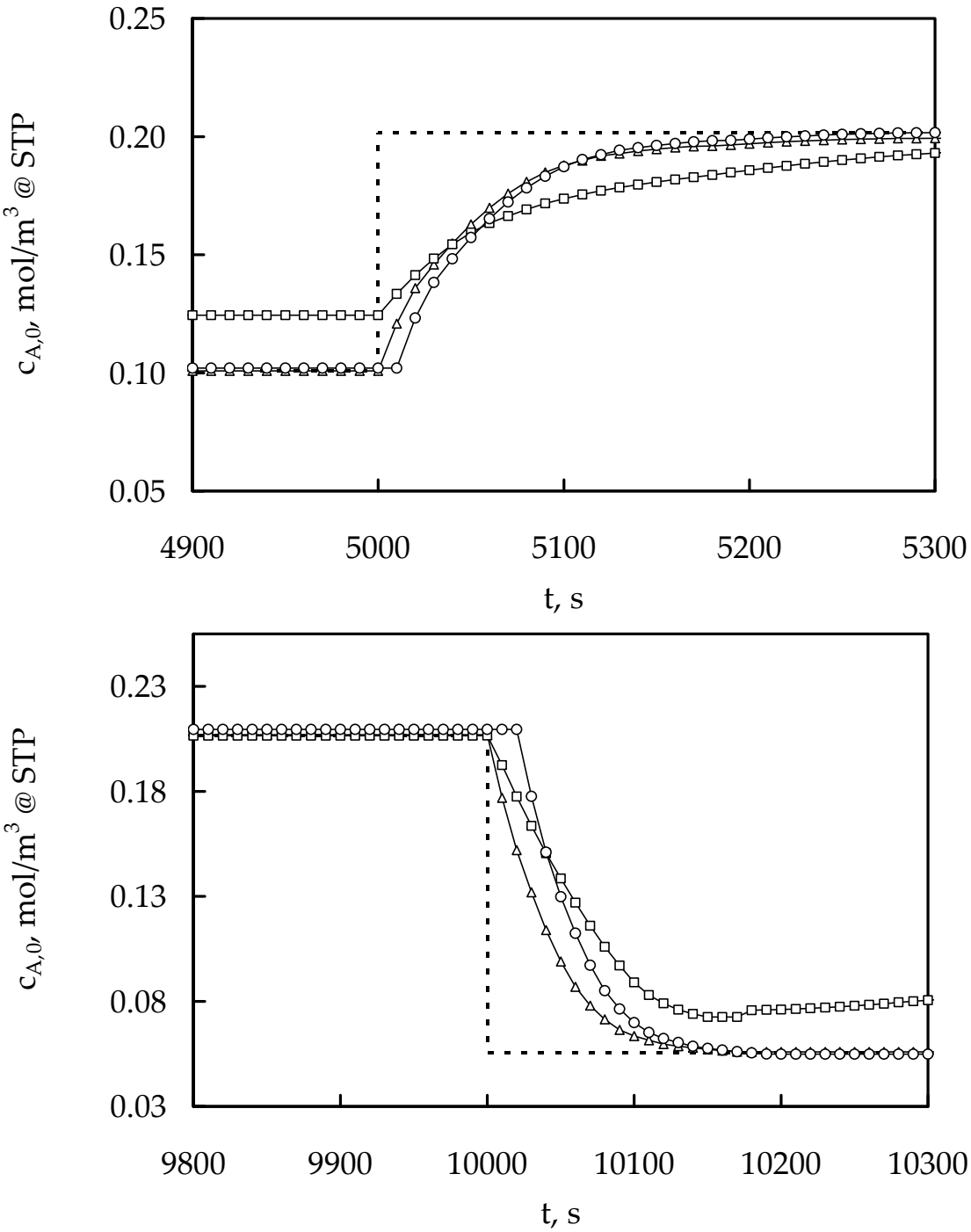
0.25
0.20
0.15
0.10
0.05
$c_{A,0}$, mol/m^3 @ STP
4900
5000
5100
5200
5300
t, s
0.23
0.18
0.13
0.08
0.03
$c_{A,0}$, mol/m^3 @ STP
9800
9900
10000
10100
10200
10300
t, s